Ion stochastic trapping and drift turbulence evolution

Madalina Vlad*
National Institute of Laser, Plasma and Radiation Physics, Bucharest, Romania

(Received 28 April 2012; revised manuscript received 2 February 2013; published 14 May 2013)

Test modes on turbulent magnetized plasmas are studied taking into account the stochastic ion trapping or eddying that characterizes the $\mathbf{E} \times \mathbf{B}$ drift in the background turbulence. It is shown that ion trapping provides an important physical mechanism for the complex nonlinear processes in drift turbulence evolution: generation of large-scale correlations and of zonal flow modes.

DOI: 10.1103/PhysRevE.87.053105 PACS number(s): 52.35.Kt, 05.10.Gg, 05.40.−a, 52.35.Ra

I. INTRODUCTION

The evolution of turbulence in magnetically confined plasmas is a complex problem that is not completely understood in spite of a huge amount of work (see Ref. [1] and the references therein). Low-frequency drift-type turbulence, which has a significant influence on plasma confinement, has been extensively studied, especially in connection with fusion research (see, e.g., Refs. [2–5]). Most of the studies that go beyond the quasilinear stage are based on numerical simulations or on simplified models. Numerical simulations show a complex nonlinear evolution with generation of large correlations, increase of order, appearance of zonal flow modes ([6,7]), and nonlinear damping of turbulence. It is interesting to note that zonal flow modes have been obtained in simulations based on different approaches (gyrokinetic [3], Hasegawa-Mima [8], and Hasegawa-Wakatani [9] models), and in different confining geometries (slab, toroidal, cylindrical), conditions (collisional or collisionless plasmas), and types of turbulence (drift, ion temperature gradient driven or trapped-electron modes). This suggests that the zonal flow mode generation is a robust process in plasma turbulence that is related to the basic physics of the nonlinear interaction. Zonal flow modes and their effects on turbulence damping and on improved confinement is presently a very active research topic ([10–15]).

The stochastic particle advection that appears in turbulent plasmas due to the $\mathbf{E} \times \mathbf{B}$ (or electric) drift can produce trajectory trapping or eddying around contour lines of the potential ([16–19]). Trapping has a strong effect on the statistics of particle trajectories. Analytical methods suitable to the study of particle stochastic advection in the presence of trapping were developed only in the last decade ([20,21]). They permitted researchers to show that trapping determines strong deviation from the Gaussian advection processes, leading to memory effects, quasicoherent behavior, and non-Gaussian distribution. The trapped trajectories have quasicoherent behavior, and they form structures similar to fluid vortices.

The aim of this paper is to contribute to the understanding of the effects of trajectory trapping on the evolution of drift turbulence. These are the first analytical results on this complex problem that are in agreement with numerical simulations. A Lagrangian approach is developed, which extends the type of methods initiated by Dupree [22,23] to the nonlinear regime characterized by trapping.

We study linear modes that develop on turbulent plasma with the statistical characteristics of the potential considered known. The basic description provided by the drift kinetic equations in the collisionless limit is used. Analytical expressions are derived, which approximate the growth rates and the frequencies of the test modes as functions of the characteristics of the background turbulence.

The characteristics of the test mode provide the tendencies in turbulence evolution. There is a sequence of processes, which appear at different stages of evolution as transitory effects. The drift turbulence has an oscillatory behavior remaining in the nonlinear stage. A different perspective on important aspects of the physics of drift-type turbulence in the strongly nonlinear regime (as zonal flow mode generation) is deduced. An important role in these processes is shown to be played by the ion stochastic trapping or eddying.

The paper is organized as follows. The dispersion relation for the drift modes on turbulent plasmas is deduced in the next section. It is shown that the effects of the background turbulence are contained in a function of time that enters in the ion propagator. It is an average over the stochastic ion trajectories in the background turbulence. The statistical methods for evaluating this function are shortly presented. The next three sections present the effects of turbulence on the test modes at different stages in turbulence evolution: quasilinear turbulence, weak nonlinear regime (when the fraction of trapped ions is small), and strong nonlinear regime (with strong trapping). The evolution of the drift turbulence is discussed at each stage. The summary of results and the conclusions are presented in the last section.

II. TEST MODES ON TURBULENT PLASMAS

Drift waves and instabilities are low-frequency modes generated in nonuniform magnetically confined plasmas. Depending on the particular conditions, there are several types of drift modes. Since the aim of this work is to understand the effects of trapping on the evolution of turbulence, we consider a simple confining geometry, the plane plasma slab, in which the magnetic field is straight and uniform. Plasma has low β, which means that the perturbation of the magnetic field is negligible (electrostatic approximation).

The magnetic field is along the z axis ($\mathbf{B} = B\mathbf{e}_z$), and plasma is nonuniform in one direction taken along the x axis. For simplicity, the equilibrium temperatures are uniform and

*madalina.vlad@inflpr.ro

only the density $n_0(x)$ is x dependent. The characteristic length of density variation $L_n = n_0/|dn_0/dx|$ is much larger than the wave length of the drift modes.

We start from the basic description of this (universal) drift turbulence provided by the drift kinetic equation in the collisionless limit. Electron kinetic effects produce the dissipation mechanism to release the energy and, combined with finite Larmor radius of the ions, make drift waves unstable. The latter consist of the polarization drift velocity and of the modification of the electric drift velocity of the ions due to the gyro-average of the potential. Both effects determine the decrease of mode frequency below the diamagnetic frequency, which makes the growth rate positive. Beside this, the polarization drift has a more complex influence determined by its nonzero divergence. We neglect here the modification of the potential and consider the effects of the polarization drift. The reason is that, as shown below, the background turbulence in the nonlinear regime eliminates the effects of the finite Larmor radius on the frequency. Thus, this approximation that determines sensible simplifications of the calculations has a negligible influence on the phenomenology of drift turbulence evolution in the nonlinear regime. Preliminary results, which take into account the gyro-average of the potential and neglect the polarization drift, are presented in Ref. [24].

Drift modes are represented by wave type potential $\delta\phi(x,y,z,t) = \phi_{k\omega}\exp(ik_x x + ik_y y + ik_z z - i\omega t)$, where k_i are the components of the wave number and ω is the frequency (with imaginary part γ). They have

$$k_z \ll k_x, k_y,\ v_{Ti} \ll \omega/|k_z| \ll v_{Te}, \tag{1}$$

where v_{Te}, v_{Ti} are the thermal velocities of electrons and ions, respectively. The solution of the dispersion relation, which is the quasineutrality condition, is (see Ref. [25])

$$\omega = \frac{k_y V_{*e}}{1 + k_\perp^2 \rho_s^2}, \tag{2}$$

$$\gamma = \sqrt{\frac{\pi}{2}}\frac{\omega(k_y V_{*e} - \omega)}{|k_z| v_{Te}}, \tag{3}$$

where $\mathbf{V}_{*e} = V_{*e}\mathbf{e}_y$, $V_{*e} = T_e/(eBL_n) = \rho_s c_s/L_n$ is the diamagnetic velocity, $\rho_s = c_s/\Omega_i$, $c_s = \sqrt{T_e/mi}$, T_e is the electron temperature, m_i is the ion mass, e is the absolute value of electron charge, $\Omega_i = eB/m_i$ is the cyclotron frequency, and $k_\perp = \sqrt{k_x^2 + k_y^2}$ is the perpendicular wave number. Usual normalized quantities $\overline{k}_i = k_i\rho_s$, $\overline{\omega} = \omega L_n/c_s$, $\overline{\gamma} = \gamma L_n/c_s$ will be used for the results, while physical quantities appear in the calculations. The normalized frequencies and growth rates for the linear drift modes are

$$\overline{\omega} = \frac{\overline{k}_y}{1 + \overline{k}_\perp^2}, \tag{4}$$

$$\overline{\gamma} = \gamma_0 \overline{\omega}(\overline{k}_y - \overline{\omega}), \tag{5}$$

where $\gamma_0 = \sqrt{\pi/2}(c_s/L_n)/|k_z|v_{Te}$. Drift modes are unstable ($\gamma > 0$) if $\overline{\omega} < \overline{k}_y$. The maximum growth rate is for $\overline{\omega} = \overline{k}_y/2$, which corresponds to $k_\perp\rho_s = 1$. The ρ_s dependence that appears in (2) yields from the ion polarization drift

$$\mathbf{u}_p = \frac{m_i}{eB^2}\partial_t \mathbf{E}_\perp. \tag{6}$$

The solution (4) and (5) in the limit $\rho_s = 0$ (obtained by neglecting the polarization drift) is $\omega = k_y V_{*e}$, $\gamma = 0$, which represents the stable drift waves. For an arbitrary initial condition ϕ_0, this solution is

$$\phi(x,y,z,t) = \phi_0(x, y - V_{*e}t, z). \tag{7}$$

It shows that any potential ϕ_0 in a nonuniform plasma moves with the diamagnetic velocity. Finite Larmor radius effects, collisions, or other perturbations determine supplementary time dependencies that modify the potential amplitude and shape, but this usually appears on a larger time scale.

This model of modes developing on quiescent plasma is not realistic because drift instabilities appear for a large range of wave numbers and produce a turbulent potential. Test mode models consider a turbulent plasma with given statistical characteristics of the background potential $\phi_b(\mathbf{x},z,t)$ and a small perturbation $\delta\phi, \phi = \phi_b + \delta\phi$. The growth rates and the frequencies of the test modes are determined as functions of the statistical characteristics of ϕ_b. The potential ϕ_b is taken as the zero ρ_s solution (7). The modification of potential shape and amplitude appears due to polarization drift on a larger time scale of the order $1/\gamma$. The test mode studies of turbulence are based on this time-scale separation, which permits a sequential approach. Starting from a potential that is a zero order solution (7), it is possible to determine the frequency and the growth rate of test modes as a function of the statistical characteristics of the potential. They provide information on the tendency in the evolution of the potential, which is used to determine the test mode properties later in the evolution, and so on.

The main statistical characteristics of the background turbulence are the amplitude β of the potential fluctuations, their correlation lengths λ_x, λ_y, and correlation time τ_c. They appear in the Eulerian correlation (EC) of the potential defined by

$$E(\mathbf{x},t) \equiv \langle \phi_b(\mathbf{x}',t')\phi_b(\mathbf{x}' + \mathbf{x}, t' + t)\rangle, \tag{8}$$

where $\langle\rangle$ is the statistical average or the space average. This function is the Fourier transform of the spectrum. The amplitude of the stochastic electric drift is $V = \sqrt{V_x^2 + V_y^2}$, where $V_x = \beta/B\lambda_y$, $V_y = \beta/B\lambda_x$. These parameters define the time of flight (or the eddying time) $\tau_{fl} = \lambda_x/V_x = \lambda_x\lambda_y B/\beta$, which is the characteristic time for trajectory trapping.

The perturbations of the electron and ion distribution functions as a response to the potential $\delta\phi$ have to be determined as functions of the EC of the background turbulence.

The electrons have the same response to a perturbation $\delta\phi$ as in quiescent plasma due to their fast parallel motion

$$\delta n^e = n_0(x)\frac{e\delta\phi}{T_e}\left(1 + i\sqrt{\frac{\pi}{2}}\frac{\omega - k_y V_{*e}}{|k_z| v_{Te}}\right) \tag{9}$$

(see, for example, Ref. [25, p. 457]).

The ion response is obtained from the drift kinetic equation

$$O^i f^i + f^i \nabla\cdot\mathbf{u}_p = 0, \tag{10}$$

$$O^i \equiv \partial_t - \frac{\nabla\phi_b \times \mathbf{b}}{B}\cdot\nabla, \tag{11}$$

where O^i is the derivative along ion trajectories where parallel motion is negligible due to condition (1). The distribution

$$f_0^i = n_0(x) F_M^i \left[1 + \frac{e\phi_b(\mathbf{x} - \mathbf{V}_{*e} t)}{T_e} \right] \tag{12}$$

represents the short time approximate equilibrium because $O^i f_0^i = 0$ and the term $\nabla \cdot \mathbf{u}_p \ll 1$. Perturbing the potential with $\delta\phi$, the operator is perturbed with

$$\delta O^i = -\frac{1}{B} \nabla \delta\phi \times \mathbf{e}_z \cdot \nabla$$

and a change of the distribution function appears: $f^i = f_0^i + h$. The linearized equation in this perturbation

$$O^i h + h \nabla \cdot \mathbf{u}_p = -i n_0(x) F_M^i \frac{e\delta\phi}{T_e} \left(k_y V_{*e} - \omega \rho_s^2 k_\perp^2 \right) \tag{13}$$

has the formal solution

$$h(\mathbf{x}, v, t) = -n_0(x) F_M^i \frac{e\delta\phi}{T_e} \left(k_y V_{*e} - \omega \rho_s^2 k_\perp^2 \right) \overline{\Pi}^i, \tag{14}$$

where the propagator is

$$\overline{\Pi}^i = i \int_{-\infty}^{t} d\tau \; M(\tau) \; \exp[-i\omega(\tau - t)] \tag{15}$$

and $M(\tau)$ is the average over ion trajectories

$$M(\tau) \equiv \left\langle \exp\left\{ i\mathbf{k}\cdot[\mathbf{x}(\tau) - \mathbf{x}] - \int_\tau^t d\tau' \; \nabla \cdot \mathbf{u}_p[\mathbf{x}(\tau')] \right\} \right\rangle. \tag{16}$$

The integrals are along ion trajectories obtained from

$$\frac{d\mathbf{x}(\tau)}{d\tau} = -\frac{\nabla\phi(\mathbf{x} - \mathbf{V}_{*e} t) \times \mathbf{e}_z}{B}, \tag{17}$$

calculated backwards in time with the condition at $\tau = t$, $\mathbf{x}(t) = \mathbf{x}$.

The last term in the argument of the exponential in Eq. (16) accounts for the compressibility effects in the background turbulence produced by the polarization drift. This term has zero average, but, as shown below, its correlation with the displacements

$$L_i(\tau) = \frac{m_i}{eB^2} \int_\tau^t d\tau'' \int_\tau^t d\tau' \langle v_i[\mathbf{x}(\tau'')] \partial_{\tau'} \Delta\phi[\mathbf{x}(\tau')] \rangle \tag{18}$$

can play an important role in the evolution of the turbulence. This is a Lagrangian correlation that has the dimension of a length and represents the effect of the compressibility in the background potential due to the polarization drift.

The dispersion relation for test modes in turbulent plasma obtained from the quasineutrality condition is

$$-\left(k_y V_{*e} - \omega \rho_s^2 k_\perp^2 \right) \overline{\Pi}^i = 1 + i \sqrt{\frac{\pi}{2}} \frac{\omega - k_y V_{*e}}{|k_z| v_{Te}}. \tag{19}$$

It is the same as in quiescent plasma, except for the function $M(\tau)$ that appears in the propagator (15).

Thus, the function $M(\tau)$ defined by Eq. (16) embeds all the effects of the background turbulence. $M(\tau)$ depends implicitly on the background potential through the statistical characteristics of the trajectories (17), which determine the average. It also depends explicitly on the background turbulence through the compressibility term L_i. In the case of quiescent plasmas $M = 1$.

This function and its evolution are estimated in the next sections. We present here a short review of the statistical methods.

The $\mathbf{E} \times \mathbf{B}$ drift in turbulent plasmas can determine trajectory trapping or eddying. It is permanent in the case of static electric fields and appears due to the Hamiltonian character of the motion with the potential ϕ as a conserved Hamiltonian. When this motion is weakly perturbed by slow time variation of the potential or by other components of the motion, trapping persists for finite time intervals determined by the strength of the perturbation [16–19].

Semianalytical statistical methods (the decorrelation trajectory method DTM [20] and the nested subensemble approach NSA [21]) have been developed for the study of test particle stochastic advection. Essentially, DTM and NSA reduce the problem of determining the statistics of the stochastic trajectories to the calculation of weighted averages of some smooth, deterministic trajectories determined from the EC of the stochastic potential. The main advantage of these methods is to be in agreement with the statistical consequences of the invariance of the potential so that they are able to describe trajectory trapping. NSA is the development of DTM as a systematic expansion that validates DTM and yields much more statistical information. These are semianalytic methods, which need PC-level computations of a few minutes. A series of studies ([21] and the references therein, [26]) have shown that trapping determines memory effects, anomalous diffusion regimes, quasicoherent behavior, and non-Gaussian distribution. The trapped trajectories form structures similar to fluid vortices. It was also shown that the trajectory structures also modify the advection process of passive scalar fields [27].

The EC of the potential is initially modeled according to the frequencies and the growth rates of drift modes in quiescent plasma (4)–(5), and then it is changed as required by the modification of these quantities in turbulent plasma. These equations show that the maximum of γ corresponds to $k_\perp \rho_s = 1$, with larger k_y (of the order of ρ_s^{-1}) and smaller k_x. The growth rate is zero for $k_y = 0$. Thus, the spectrum of the drift type turbulence is zero along the line $k_y = 0$, which means that the integral of the EC along y must be zero. It has two peaks at $k_y = \pm k_0, k_x = 0$. A simple analytical approximation for the spectrum is

$$S(\mathbf{k}) \sim k_y \exp\left(-\frac{k_x^2}{2} \lambda_x^2 \right) \left\{ \exp\left[-\frac{(k_0 - k_y)^2}{2} \lambda_y^2 \right] - \exp\left[-\frac{(k_0 + k_y)^2}{2} \lambda_y^2 \right] \right\}, \tag{20}$$

which corresponds to the EC,

$$E(\mathbf{x}, t) = \beta^2 \partial_y \left[\exp\left(-\frac{x^2}{2\lambda_x^2} - \frac{y'^2}{2\lambda_y^2} \right) \frac{\sin k_0 y'}{k_0} \right], \tag{21}$$

where $y' = y - V_{*e} t$, λ_i and the dominant wave number k_0 are of the order 1.

Starting from the EC (21), the statistics of ion trajectories is determined, then the function $M(\tau)$, the averaged ion propagator, the growth rate and the frequency of the drift modes are estimated. These quantities show how the EC evolves.

The distribution of displacements obtained from Eqs. (17) strongly depends on the ordering of the characteristic times of the stochastic process. The longest characteristic time is the parallel time of the ions $\tau_{\|i} = \lambda_{\|}/v_{Ti}$, which actually leads to negligible parallel motion. The motion of the potential along y with the diamagnetic velocity defines the diamagnetic time $\tau_* = \lambda_y/V_{*e}$. The correlation time of the potential τ_c, which is the characteristic time for the change of the shape of the potential, is of the order $\tau_c \cong \gamma^{-1}$. Thus, it is larger than the diamagnetic time ($\tau_c > \tau_*$). The time of flight (or eddying time) is defined by $\tau_{fl} = \lambda_y/V_y = B\lambda_x\lambda_y/\beta$. Trajectory trapping appears when τ_{fl} is smaller than τ_*. The trapping parameter for drift turbulence is

$$K_* = \tau_*/\tau_{fl} = V_y/V_{*e} = \beta/(\lambda_x V_{*e} B) \tag{22}$$

(not the Kubo number $K = \tau_c/\tau_{fl}$) because the decorrelation is produced by potential motion. Trajectory trapping exists when $K_* > 1$. The fraction of trapped trajectories n_{tr} and the maximum size of trajectory structures are increasing functions of K_*.

The average propagator (15) is calculated in the next sections using simplified models that include the main characteristics of the probability of displacements. It is thus possible to capture the complicated nonlinear effects of strong turbulence in rather simple analytical expressions. The results can easily be improved by taking into account the statistics of test particles obtained with the nested subensemble method. This significantly more complicated approach that relies on numerical calculation of the averages does not change qualitatively the results. We consider that the simple analytical expressions derived in the next sections give a more clear image on the complex nonlinear processes that appear in the drift turbulence evolution beyond the quasilinear stage.

III. ION DIFFUSION AND DAMPING OF LARGE *k* MODES

For small amplitude of the background potential, the time of flight is larger than the decorrelation time ($K_* < 1$), and trapping does not appear. The smallest characteristic time that influences the ion motion corresponds to the potential motion with the diamagnetic velocity. The characteristic times ordering is

$$\tau_{\|e} < \tau_* < \tau_c < \tau_{fl} < \tau_{\|i}. \tag{23}$$

This corresponds to small amplitude background turbulence with $\beta/B \ll V_{*e}\lambda_x$.

The diffusion coefficients D_i, $i = x,y$ determined for the EC (21) are very small in both directions, much smaller along y than for a monotonically decaying potential. The distribution of the displacements is Gaussian, and it leads to

$$M(\tau;t) = \exp\left[-\frac{k_i^2\langle[x_i(\tau)-x_i]^2\rangle}{2} + ik_iL_i\right], \tag{24}$$

where $L_i(\tau)$ is defined in Eq. (18), and the small quadratic term in the divergence of the polarization drift was neglected.

The trajectories (the characteristics) have displacements until decorrelation by potential motions that are small compared to the correlation length and can be neglected. This strongly simplifies the estimation of the compressibility term L_i because the Lagrangian correlation in (18) can be approximated by the corresponding Eulerian correlations. The correlation in L_x can be approximated by

$$\langle v_x(\tau'')\partial_{\tau'}\Delta\phi(\tau')\rangle \cong \frac{1}{V_{*e}}\partial_{\tau''}\partial_{\tau'}\Delta E[\mathbf{V}_{*e}(\tau''-\tau')],$$

where $v_x(\tau) \equiv v_x(\mathbf{x} - \mathbf{V}_{*e}(t-\tau))$. The time integral yields

$$L_x(\tau) = \frac{2}{BV_{*e}}(\Delta E(\mathbf{0}) - \Delta E[\mathbf{V}_{*e}|t-\tau|)], \tag{25}$$

which is finite because the Laplacean of the EC is symmetrical and finite in zero. This function of time starts from zero at the time $\tau = t$ and saturates in a time of the order of τ_* at the value $-2V^2/BV_{*e}$.The component L_y is zero because it contains one or three derivatives at x for $x = 0$, which are zero.

Thus in the quasilinear case

$$M = \exp\left[-k_i^2D_i(t-\tau) - i2k_x\frac{V^2}{\Omega_iV_{*e}}\right], \tag{26}$$

which shows that the compressibility determines a constant term proportional with the square of the amplitude of the stochastic velocity determined by the background turbulence. This is very small due to Ω_i and to the condition $V \ll V_{*e}$ imposed for this regime.

The propagator is

$$\overline{\Pi}^i = -\exp\left[-i2k_x\frac{V^2}{\Omega_iV_{*e}}\right]\frac{1}{\omega + ik_i^2D_i} \tag{27}$$

and the ion density perturbation

$$\delta n^i(\mathbf{x},v,t) = n_0(x)\frac{e\delta\phi}{T_e}A\frac{k_yV_{*e} - \omega\rho_s^2k_\perp^2}{\omega + ik_i^2D_i}, \tag{28}$$

where

$$A = \exp\left[-i2k_x\frac{V^2}{\Omega_iV_{*e}}\right] \approx 1 - i2k_x\frac{V^2}{\Omega_iV_{*e}}. \tag{29}$$

This factor produced by the polarization drift is very close to unity.

The solution of the dispersion relations is

$$\overline{\omega} = \frac{\overline{k}_y}{1+\overline{k}_\perp^2}, \tag{30}$$

$$\overline{\gamma} = \gamma_0\overline{\omega}(\overline{k}_y - \overline{\omega}) - \overline{k}_i^2\overline{D}_i - 2\overline{k}_x\overline{\omega}\frac{V^2}{\rho_sc_s}, \tag{31}$$

where $\overline{D}_i = D_i/(\rho_sV_{*e})$. Thus, the frequency is not influenced by the background turbulence when it has small amplitude. The latter determines new terms in the growth rate.

The main effect is produced by ion trajectory diffusion in the background turbulence, which determine the damping of the modes with large k (the second term in γ). This is the well-known result of Dupree, which is recovered here. An additional effect is obtained from the compressibility, which determines the asymmetrical increase of the modes (contribution to the growth of the modes with $k_xk_y < 0$ and to the decay of those with $k_xk_y > 0$). This effect is very small because the ratio of the third term to the first term in Eq. (31) is of the order $(1/\Omega_i\tau_{\|e})(V^2/V_{*e}^2) \ll 1$.

The frequency and the growth rate of the modes on turbulent plasma with small amplitude show that the most unstable modes are, as in quiescent plasma, those with $\omega \cong k_y V_{*e}/2$, which have wave numbers of the order of ρ_s^{-1} ($\overline{k}_\perp^2 \cong 1$). Their interaction with the background turbulence is weak, except for the large k modes, which decay and eventually are damped due to ion diffusion.

This means that the EC of the turbulence evolves in this quasilinear stage by increasing its amplitude β without major change of its shape.

IV. TRAJECTORY STRUCTURES AND LARGE-SCALE CORRELATIONS

The increase of the amplitude β of the stochastic potential determines the change of the ordering of the characteristic times (23). When V becomes larger than the velocity of the potential V_{*e} (or $\beta/B > V_{*e}\lambda_x$), the time of flight is smaller that the decorrelation time τ_*

$$\tau_\parallel^e \ll \tau_{fl} < \tau_* \ll \tau_c \ll \tau_\parallel^i \tag{32}$$

and $K_* > 1$. In these conditions ion trapping or eddying appears. As we have shown, this strongly influences the statistics of trajectories. The distribution of the trajectories is not Gaussian any more due to trapped trajectories that form quasicoherent structures. At this stage the trapping is weak in the sense that the fraction of trapped trajectories n_{tr} is much smaller than the fraction n_f of free trajectories.

The probability of displacements $P(\mathbf{x},t)$ was obtained using the nested subensemble method. It has a pronounced peaked shape compared to the Gaussian probability. The contribution of the trapped particles to the probability $P(\mathbf{x},t)$ at time t appears as a narrow peak in $r = 0$, which remains invariant after formation. The time invariance of this central part of the probability is due to the vortical motion of the trapped particles. It shows that vortical structures appear due to trapping. The size of the vortical structure depends on the strength of the decorrelation mechanism that releases the trapped particles. The free particles, for which the motion is essentially radial, determine the larger distance part of the probability, which continuously extends. The probability of displacements until decorrelation ($\tau < \tau_*$) is modeled by

$$P(x,y,\tau) = n_{tr} G(\mathbf{x};\mathbf{S}) + n_f G(\mathbf{x};\mathbf{S}'), \tag{33}$$

where $G(\mathbf{x};\mathbf{S})$ is the two-dimensional Gaussian distribution with dispersion $\mathbf{S} = (S_x,S_y)$. The first term describes the trapped trajectories. We have considered for simplicity their distribution as a Gaussian function, but with small (fixed) dispersion that represents the square of the average size s_i of the structures $S_i = s_i^2$. The shape of this function does not change much the estimations. The free trajectories are described by the second term in Eq. (33). They have dispersion that grows linearly in time: $S_i'(\tau) = S_i + 2D_i(t-\tau)$, $i = x,y$. The initial value $S_i'(t) = S_i$ is an effect of trapping. It essentially means that the trajectories are spread over a surface of the order of the size of the trajectory structures when they are released by a decorrelation mechanism.

The compressibility term L_i will be calculated in the next section. As shown there, it is negligible in these conditions.

The propagator, obtained by performing the average in Eq. (16) using the probability (33), is

$$\overline{\Pi}^i = -\frac{1}{\omega + i k_i^2 D_i}\mathcal{F}, \tag{34}$$

where the factor $\mathcal{F}$ is determined by the average size of the trapped trajectory structures

$$\mathcal{F} \equiv \exp\left(-\frac{1}{2}k_i^2 S_i\right). \tag{35}$$

The solution of the dispersion relation (19) is

$$\overline{\omega} = \frac{\mathcal{F}\overline{k}_y}{1+\mathcal{F}\overline{k}_\perp^2}, \tag{36}$$

$$\overline{\gamma} = \gamma_0 \overline{\omega}(\overline{k}_y - \overline{\omega}) - \overline{k}_i^2 \overline{D}_i. \tag{37}$$

Thus, the effect of trajectory trapping appears in the frequency while the growth rate is not modified (the small compressibility term was neglected).

Trajectory trapping determines the decrease of the frequency. The value of $k_\perp$ corresponding to the maximum of γ (at $\overline{\omega} = \overline{k}_y/2$) is displaced from values $\overline{k}_\perp \cong 1$ to $\overline{k}_\perp \cong 1/s$ where $s = \sqrt{S_x + S_y}/\rho_s$ is the size of trajectory structures normalized with ρ_s. For $s \gg 1$ ($S_i \gg \rho_s^2$), the frequency (36) is $\overline{\omega} \cong \mathcal{F}\overline{k}_y$, which shows that the finite Larmor radius effects become negligible in the presence of trapping when the size of the vortical structures is larger than ρ_s.

The growth rates of the drift modes for different values of s are shown in Fig. 1. One can see the displacement of unstable mode range toward small $k_\perp$. This determines a further increase of the size of trajectory structures. The process is accompanied by the decrease of the growth rates.

This means that the EC of the turbulence evolves in this weakly nonlinear stage by continuing the increase of the amplitude β (at smaller rate) and by the increase of

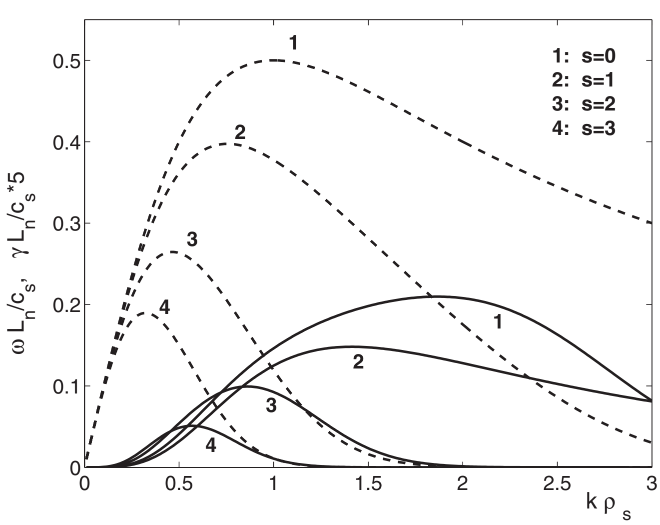

FIG. 1. The frequencies (36) (dashed lines) and the growth rates (37) (continuous lines) of the drift modes in the weakly nonlinear regime for several values of the size of trajectory structures. The displacement of the unstable domain towards small k and the decrease of the growth rate appear when s increases. $\overline{\gamma}$ is multiplied with the factor 5.

the correlation length. The dominant wave number k_0 (21) decreases. The vortical structures of ion trajectories produced by trapping determine this process of generating large-scale correlations and of slowing down the evolution (compared to the quasilinear stage).

V. EFFECTS OF THE ION FLOWS

The evolution of the potential determines the increase of the fraction of trapped ions. As n_{tr} increases, the average flux of the trapped particles that move with the potential $n_{tr}V_{*e}$ becomes important. Since the $\mathbf{E}\times\mathbf{B}$ drift has zero divergence, the probability of the Lagrangian velocity is time invariant; i.e., it is the same with the probability of the Eulerian velocity. The average Eulerian velocity is zero, and thus the flux of the trapped ions that move with the potential has to be compensated by a flux of the free particles. These particles have an average motion in the opposite direction with a velocity V_f such that

$$n_{tr}V_{*e} + n_f V_f = 0. \quad (38)$$

The NSA shows that the probability of the displacements splits in two components that move in opposite direction. The peak of trapped ions moves with the velocity V_{*e} while the free ions move in the opposite direction with a velocity that increases with the increase of the fraction of trapped ions $V_f = -nV_{*e}$, where $n = n_{tr}/n_f$. The distribution of trapped ions is almost frozen while that of free ions has a continuously growing width. Thus, opposite ion flows are generated by the moving potential in the presence of trapping. A simple approximation that includes the main features of the distribution is

$$P(x,y,t) = n_{tr}G(x,y - V_{*e}t;\mathbf{S}) + n_f G(x,y - V_f t;\mathbf{S}'), \quad (39)$$

where two Gaussian functions were used as in Eq. (33) but taking into account the ion flows (38). The separation of the distribution and the existence of ion flows in drift-type turbulence are confirmed by numerical simulations [28].

The compressibility term L_i (18) is determined for trapped and free particles with the DTM. The component L_y is zero for both trapped and free ions due to the symmetry. L_x is different for free and trapped trajectories. In the first case there is a relative motion of the free ions and of the potential with the velocity V_{*e}/n_f [obtained from (38)], which determines rapid decorrelation. The estimation done for the quasilinear turbulence also holds in these conditions, and L_x for free ions is approximated by Eq. (25) with V_{*e} replaced by V_{*e}/n_f, and thus it is negligible. For the trapped trajectories, L_x is much larger than in the quasilinear case. It can be written as

$$L_x = -\frac{V_{*e}}{\Omega_i B^2}\int_\tau^t d\tau''\int_\tau^t d\tau' \langle \partial_y\phi[\mathbf{x}(\tau'')]\partial_y\Delta\phi[\mathbf{x}(\tau')]\rangle,$$

where the time derivative was replaced by the y derivative since the argument is $y - V_{*e}\tau$. A nonzero value is obtained for L_x essentially because the potential and the Laplacean of the potential are correlated in a stochastic field: the maxima of the potential statistically coincide with the minima of the Laplacean. It follows that the derivatives of these functions along the same directions are also correlated, and the derivatives on different directions are not. L_x can be determined with the DTM, which shows that the following estimation holds:

$$L_x(\tau,t) = -\frac{V_{*e}}{\Omega_i B^2}\int_\tau^t d\tau''\int_\tau^t d\tau' C_x(|\tau''-\tau'|),$$
$$C_x(|\tau''-\tau'|) = \langle \partial_y\phi(\tau'')\partial_y\Delta\phi(\tau')\rangle,$$

where $\phi(\tau)\equiv\phi(\mathbf{x}(\tau) - V_{*e}(t-\tau))$.The integral is calculated by changing the integration variable τ'' to $\theta = \tau''-\tau'$:

$$L_x(\tau,t) = -\frac{2V_{*e}}{\Omega_i B^2}\int_0^{t-\tau} d\theta C_x(|\theta|)(t-\tau-\theta),$$

which integrated by parts gives

$$L_x(\tau,t) = -\frac{2V_{*e}}{\Omega_i B^2}\int_0^{t-\tau} d\theta J(\theta),$$

where

$$J(\theta) = \int_0^\theta d\tau C_x(\tau).$$

This function saturates after the decorrelation time, which is the time of flight τ_{fl} at $J = C_x(0)\tau_{fl}$. Thus

$$L_x(\tau,t) \cong a(t-\tau), \quad (40)$$

$$a = 2\partial_y^2\Delta E(\mathbf{0})\frac{\tau_{fl}V_{*e}}{\Omega_i B^2}, \quad (41)$$

where $\partial_y^2\Delta E(\mathbf{0}) = \beta^2/\lambda_y^4[(k_0^2+3)\delta + 15 + 10k_0^2 + k_0^4]$ and $\delta = \lambda_x^2/\lambda_y^2$. The factor a has the dimension of a velocity. This type of Lagrangian correlation corresponds to the decorrelation by mixing.

Thus, the compressibility of the background turbulence influences the propagator for the trapped ions. The function M (16) that accounts for the effects of the background turbulence is determined using Eqs. (39) and (40):

$$M = n_f \exp\left\{-\frac{k_i^2}{2}[S_i + 2D_i(t-\tau)] - ik_yV_f(t-\tau)\right\} + n_{tr}\exp\left[-\frac{k_i^2}{2}S_i - ik_yV_{*e}(t-\tau) + ik_x a(t-\tau)\right]. \quad (42)$$

The average propagator becomes

$$\overline{\Pi}^i = -\mathcal{F}\left[\frac{n_f}{\omega - k_yV_f + ik_i^2D_i} + \frac{n_{tr}}{\omega - k_yV_{*e} + k_x a}\right]. \quad (43)$$

The effect of the compressibility term $k_x a$ is measured by the ratio $k_x a/k_y V_{*e}$, which, for a typical plasma with $c_s = 10^6$m/s, $\beta = 150$V, $B = 3$T, $\lambda = 10^{-2}$m, $\rho_s = 2\ 10^{-3}$m, is of the order 0.05 for $k_y \cong k_x$ and diverges when $k_y \to 0$. It means that the compressibility term can be neglected for modes with $k_y \gtrsim k_x$ and that it is important for modes with $k_y \to 0$.

The solution of the dispersion relation is determined for the two cases: $k_y \gtrsim k_x$, which corresponds to drift modes, and $k_y = 0$, which are modes with different characteristics called zonal flow modes.

A. Ion flows and drift mode damping

Straightforward calculations with the propagator (43) and $a \cong 0$ lead to the solution of the dispersion relation for $k_y \gtrsim k_x$:

$$\overline{\omega}_d = \frac{1}{2}\left[\overline{\omega}_0 + (1-n)\overline{k}_y + sg\sqrt{\overline{\omega}_n^2 + \frac{4n\overline{k}_y^2}{1+\mathcal{F}\overline{k}_\perp^2}}\right], \tag{44}$$

where $n = n_{tr}/n_f$, $\overline{\omega}_n = \overline{\omega}_0 + (n-1)\overline{k}_y$, $\overline{\omega}_0$ is the frequency (36) obtained for $n \to 0$ and $sg = sign\,(\overline{\omega}_n)$. A jump appears in the frequency at $k_\perp = k_d$, which is the solution of $\overline{\omega}_0 = (1-n)\,\overline{k}_y$, which exists if $n < 1$. k_d is an increasing function of n. In the limit of large k, $\overline{\omega}_d \to -n\overline{k}_y$ if $n < 1$ and $\overline{\omega}_d \to \overline{k}_y$ if $n > 1$. This means that the asymptotic phase velocity is in the ion diamagnetic direction when $n < 1$ and in the electron diamagnetic direction when trapping is stronger such that $n > 1$.

The imaginary part (for $\overline{\gamma}_d \ll \overline{\omega}_d$) is

$$\overline{\gamma}_d = \frac{\gamma_0(\overline{\omega}_d + n\overline{k}_y)[(1-n)\overline{k}_y - \overline{\omega}_d] - n_f\overline{k}_i^2\overline{D}_i}{[(1-n)\overline{k}_y - \overline{\omega}_d]^2(1+\mathcal{F}\overline{k}_\perp^2) + n\overline{k}_y^2}(\overline{k}_y - \overline{\omega}_d)^2. \tag{45}$$

The growth rates are presented in Fig. 2. The jump in the frequency corresponds to a jump in the growth rate from negative (at small k) to positive values. Thus, the large wave-length modes are stabilized by the ion flows, while the small wave-length modes still grow. This leads to further increase of the turbulence amplitude accompanied by the decrease of its correlation length. Both effects contribute to the increase of K_*, which leads to the increase of n. Consequently, the increase of the amplitude of the turbulence continues as well as the decrease of the correlation length. The process is stopped when $n > 1$ because the growth rate becomes negative for the whole wave number range. This determines the decrease of n and the attenuation of the ion flows.

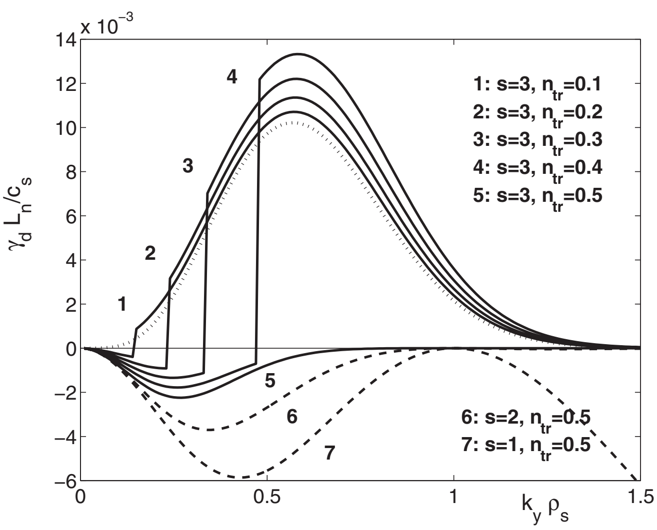

FIG. 2. The growth rates of drift modes in the strongly nonlinear regime (45) for the values of n_{tr} and of the size s of the trajectory structures that label the curves. As n_{tr} increases, $\overline{\gamma}_d$ becomes negative, first for small wave numbers and eventually for all modes. The dotted line corresponds to $n_{tr} \cong 0$.

B. Ion flows and zonal flow modes

The compressibility term determines unstable modes completely different of the drift modes: with $k_y = 0$, $k_x \neq 0$ and very small frequencies, much smaller than the diamagnetic frequency. These are called zonal flow modes. The solution of the dispersion relation (19) for $k_y = 0$ is

$$\overline{\omega}_{zf} = -\overline{k}_x\overline{a}\frac{1+\mathcal{F}\overline{k}_x^2 n_f}{1+\mathcal{F}\overline{k}_x^2}, \tag{46}$$

$$\overline{\gamma}_{zf} = \frac{n_{tr}\mathcal{F}\overline{k}_x^2\left[\gamma_0\overline{\omega}_{zf}^2 - n_f\mathcal{F}\overline{k}_x^4\overline{D}_x\right]}{\left(1+n_f\mathcal{F}\overline{k}_x^2\right)\left(1+\mathcal{F}\overline{k}_x^2\right)}, \tag{47}$$

where $\overline{a} = a/V_{*e}$. The growth rate is positive for any k_x and the frequency is small (typically ten times smaller than the diamagnetic frequency). These unstable zonal flow modes are the consequence of trapping combined with the polarization drift. One can see that when trapping is negligible ($n_{tr} \cong 0$), $\omega_{zf} = -k_x a$ and $\gamma_{zf} = 0$, and that $\omega_{zf}, \gamma_{zf} = 0$ for $\overline{a} = 0$.

The growth rates of the zonal flow modes (47) increase with the increase of n_{tr} and with the decrease of the size of the trajectory structures (see Fig. 3).

Ion diffusion effect on the zonal flow modes is negligible for large k_x due to the factor $\mathcal{F}$ that goes to zero, and it is strongest for the modes with $k_x \cong \sqrt{1/S_x}$, which can be stabilized.

C. Turbulence evolution

Thus, the ion flows produced by ion trapping in the moving potential determine two parallel effects: nonlinear damping of drift modes and generation of zonal flow modes. There is no causality relation between zonal flow modes and drift turbulence damping. Both effects are generated self-consistently in the nonlinear evolution of drift turbulence. The

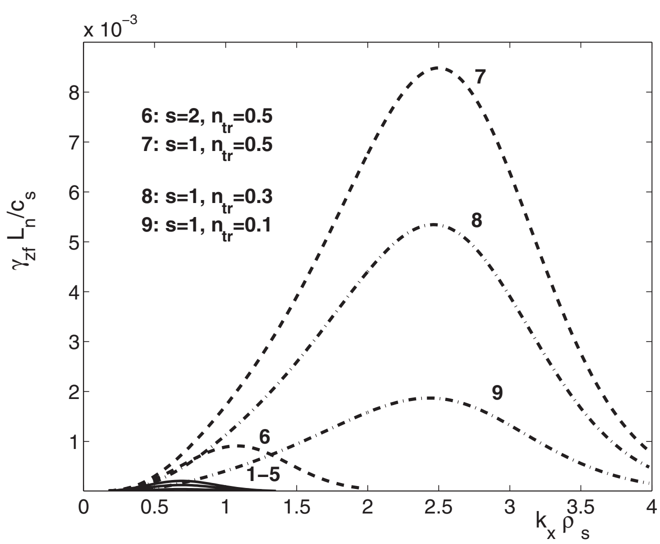

FIG. 3. The growth rates of the zonal flow modes (47) for the values of n_{tr} and of the size s of the trajectory structures that label the curves. The curves 1–5 correspond to the parameters in Fig. 2 for the same labels and show that the zonal flow modes are mostly not excited during the growth of drift modes. $\overline{\gamma}_{zf}$ strongly increases when the correlation length of the drift turbulence decreases (curves 6, 7), and it decays when drift modes are damped (curves 8, 9).

influence produced by the zonal flows on the drift type modes is only indirect, through the diffusive damping. Zonal flows modify the configuration of the potential and consequently the EC, which determines a rather strong increase of D_y and the decrease of D_x (due to the decrease of λ_x). Drift mode damping determines the decrease of $\overline{\gamma}_{zf}$ through the decrease of n_{tr}. Thus, the predator-prey paradigm [7] is not sustained by these results, although there is time correlation between the maximum growth rate of zonal flow modes and the damping of the drift modes. This time correlation can be deduced from Figs. 2 and 3, which show the growth rates of the drift and zonal flow modes for the same set of parameters n, s.

The evolution of the turbulence in this strongly nonlinear stage is rather complex. The ion flows determine first the increase of the amplitude of the turbulence and the decrease of the correlation length λ_y, then a major modification of the EC shape appears due to generation of zonal flow modes, and eventually the turbulence is strongly attenuated. The new component that accounts for the zonal flow modes adds to the EC a function with a slow decay along y ($k_y \cong 0$), with zero integral along x (because $\gamma_{zf} = 0$ for $k_x = 0$) and with amplitude growing with the increase of n. It essentially determines in the total EC the increase of λ_y and β and the decrease of λ_x.

VI. SUMMARY AND CONCLUSIONS

Test modes on turbulent plasmas were studied taking into account the process of ion trajectory trapping in the structure of the background potential. The case of drift turbulence was considered, and the frequency ω and the growth rate γ were determined as functions of the statistical properties of the background turbulence. The main characteristics of the drift turbulence evolution were deduced from γ and ω.

A different physical perspective on the nonlinear evolution of drift turbulence is obtained. The trapping of the ions in the stochastic potential that moves with the diamagnetic velocity plays a very important role. The dimensionless parameter K_* (22) that accounts for ion trajectory trapping is shown to be the main parameter which defines the stage in the evolution of drift turbulence.

Drift turbulence develops in the initial stage on a wide range of wave numbers according to the quasilinear frequencies and growth rates [(30) and (31)]. Ion trajectories are not trapped at these small amplitudes of the background turbulence, and they have a Gaussian distribution. Their diffusion determines the damping of the large **k** modes. The correlation lengths ρ_i and the inverse of the dominant wave number k_0 remain during this stage close to ρ_s. Turbulence amplitude β increases (with the largest growth rate) and the shape of the EC is not changed.

When the amplitude reaches values that make $K_* > 1$, ion trajectory trapping appears and generates vortical structures of trapped ions. They determine the decrease of the frequencies (36), which leads to the decrease of γ and to the displacement of the unstable range of wave numbers to small values of the order $1/s$, where s is the average size of trajectory structures. Turbulence amplitude continues to increase in this stage, but with a smaller rate and large-scale correlations are generated. The shape of the EC (21) remains approximately the same, and its parameters β, λ_i, $1/k_0$ increase.

When the fraction of trapped ions n_{tr} becomes comparable with the fraction of free ions n_f, ion zonal flows become important both for trajectory statistics and for test mode characteristics. Trapped ions move with the potential while free ions move in the opposite direction with the velocity $V_f = -V_{*e} n_{tr}/n_f$ such that the total flux is zero. This determines the splitting of the distribution of ion displacement and an essential change of the test modes, which consists of two effects: turbulence attenuation and generation of zonal flow modes. The attenuation of the drift modes is determined by the ion flows. It begins with the damping of small k modes, and it extends to the entire spectrum as n_{tr} increases (the growth rates are negative for the entire range of **k** at $n_{tr} = 1/2$.) A new type of modes appear in this strongly nonlinear regime, the zonal flow modes with $k_y = 0$ and very small frequencies. They are produced by the combined action of the ion flows and of the compressibility due to the polarization drift in the background turbulence. The damping of the drift modes is not determined by the zonal flows. There is only an indirect contribution through the diffusive damping, which is increased by the zonal flow modes. They modify the correlation of the turbulence by introducing components with $k_y = 0$ in the spectrum, which determine a strong increase of D_y. The decay of the drift turbulence determines the decrease of n_{tr} and consequently the decrease of the growth rate of the zonal flow modes (47).

It is interesting to underline that the growth and the decay of turbulence are produced on different paths (hysteresis process). Large scales are generated at the increase of turbulence amplitude when trapping is weak. Later in the nonlinear evolution when trapping is stronger and produces ion flows, turbulence amplitude continues to increase but accompanied by the decrease of the correlation length and by the generation of zonal flow modes. Then, when $n_{tr} \simeq 1/2$ both components of the turbulence are attenuated until the weakly nonlinear regime is attained (n_{tr} becomes small and the ion flows are negligible). A closed evolution curve in the (β,λ) space is described by the turbulence, which remains in the nonlinear stage characterized by trapping and oscillates between weak and strong trapping. The characteristic time Δt for turbulence and transport oscillations can be estimated as the inverse of the growth rates, which are of the order of $5\ 10^{-3} c_s/L_n$. One obtains for $R_0/L_n = 5$, $\Delta t = 40\ R_0/c_s$, in agreement with numerical simulations.

ACKNOWLEDGMENTS

This work was supported by CNCSIS-UEFISCDI, project numbers PNII–IDEI 1104/2008 and 4-ERC.

[1] J. A. Krommes, Phys. Rep. **360**, 1 (2002).
[2] W. Horton, Rev. Mod. Phys. **71**, 735 (1999).
[3] X. Garbet, Y. Idomura, L. Villard, and T. H. Watanabe, Nucl. Fusion **50**, 043002 (2010).
[4] G. R. Tynan, A. Fujisawa, and G. McKee, Plasma Phys. Controlled Fusion **51**, 113001 (2009).
[5] P. H. Diamond, A. Hasegawa, and K. Kima, Plasma Phys. Controlled Fusion **53**, 124001 (2011).

[6] P. W. Terry, Rev. Mod. Phys. **72**, 109 (2000).

[7] P. H. Diamond, S.-I. Itoh, K. Itoh, and T. S. Hahm, Plasma Phys. Controlled Fusion **47**, R35-R161 (2005).

[8] A. Hasegawa and K. Kima, Phys. Fluids **21**, 87 (1978).

[9] A. Hasegawa and M. Wakatani, Phys. Rev. Lett. **59**, 1581 (1987).

[10] T. Estrada, C. Hidalgo, T. Happel, and P. H. Diamond, Phys. Rev. Lett. **107**, 245004 (2011).

[11] P. Xanthopoulos, A. Mischchenko, P. Helander, H. Sugama, and T.-H. Watanabe, Phys. Rev. Lett. **107**, 245002 (2011).

[12] M. Xu *et al*., Phys. Rev. Lett. **108**, 245001 (2012).

[13] L. Schmitz, L. Zeng, T. L. Rhodes, J. C. Hillesheim, E. J. Doyle, R. J. Groebner, W. A. Peebles, K. H. Burrell, and G. Wang, Phys. Rev. Lett. **108**, 155002 (2012).

[14] Z. Guo, L. Chen, and F. Zonca, Phys. Rev. Lett. **103**, 055002 (2009).

[15] P. Manz, M. Ramisch, and U. Stroth, Phys. Rev. Lett. **103**, 165004 (2009).

[16] R. H. Kraichnan, Phys. Fluids **19**, 22 (1970).

[17] R. Balescu, *Aspects of Anomalous Transport in Plasmas* (Institute of Physics Publishing, Bristol, 2005).

[18] M. Neuer and K. H. Spatschek, Phys. Rev. E **74**, 036401 (2006).

[19] W. D. McComb, *The Physics of Fluid Turbulence* (Clarendon, Oxford, 1990).

[20] M. Vlad, F. Spineanu, J. H. Misguich, and R. Balescu, Phys. Rev. E **58**, 7359 (1998).

[21] M. Vlad and F. Spineanu, Phys. Rev. E **70**, 056304 (2004).

[22] T. H. Dupree, Phys. Fluids **9**, 1773 (1966).

[23] T. H. Dupree, Phys. Fluids **15**, 334 (1972).

[24] M. Vlad and F. Spineanu, Romanian J. Phys. **56**(Supp.), 23 (2011).

[25] R. J. Goldstone and P. H. Rutherford, *Introduction to Plasma Physics* (Institute of Physics Publishing, Bristol, 1995).

[26] M. Vlad, F. Spineanu, and S. Benkadda, Phys. Rev. Lett. **96**, 085001 (2006).

[27] M. Vlad, F. Spineanu, and S. Benkadda, Plasma Phys. Controlled Fusion **50**, 065007 (2008).

[28] T. Hauff and F. Jenko, Phys. Plasmas **14**, 092301 (2007).